Available online at www.sciencedirect.com
ScienceDirect
Journal of Power Sources 158 (2006) 1039–1046
JOURNAL OF POWER SOURCES
www.elsevier.com/locate/jpowsour

Internal battery temperature estimation using series battery resistance measurements during cold temperatures

A. Hande *

Electrical and Computer Engineering Department, Lake Superior State University, 650 West Easterday Avenue, Sault St. Marie, MI 49783, United States

Available online 27 December 2005

Abstract

A technique has been developed to estimate the internal battery temperature (T_{bat}) of secondary batteries by measuring the series battery resistance (R_B) at cold ambient temperatures. Tests were performed on both lead-acid and nickel metal hydride batteries at different cold temperatures to obtain useful plots of R_B versus T_{bat}. R_B was measured by using a pulse discharge circuit to apply a short-duration current pulse (I_B) directly to the battery. The test results indicated that R_B not only varies with temperature but also varies with the amplitude of I_B. The R_B versus T_{bat} plots were later utilized to predict T_{bat} from R_B during alternating current (AC) battery heating at cold ambient temperatures.

Keywords: Battery temperature; Battery resistance; Alternating current; Battery heating; Cold temperatures; Lead-acid

1. Introduction

In order to improve the performance of series battery packs at cold temperatures, their electrolyte needs to be warmed up. Although several external heating strategies can be used, these methods add considerable weight and expense. Moreover, if the pack is allowed to reach a very low temperature, these methods require significant amount of time for warming the batteries since the external heat energy must penetrate the large mass of the pack. Internal heating strategies, such as circulating alternating currents (AC) at high frequencies to heat batteries via I^2R losses seem to be a viable alternative [1–4]. This strategy has produced very encouraging preliminary results and the effect of these currents on overall battery life is currently being studied.

No matter what technique is used for heating secondary batteries, it is imperative that their electrolyte temperature be monitored as they warm up [5]. This is necessary because overheating can damage a battery beyond repair. It is quite easy to measure the battery case temperature (T_x) but this does not provide a good estimate of the electrolyte temperature (T_{bat}). It is therefore, necessary to monitor T_{bat} rather than T_x. This is possible by inserting a thermocouple or a thermistor within the battery case during manufacture. However, at present, battery manufacturers have not been doing this, and therefore, an alternate technique is required to monitor T_{bat}. Fortunately, the series battery resistance, R_B, varies with the internal battery temperature and therefore, this parameter can be used to monitor T_{bat}.

2. Cold temperature battery performance

At cold temperatures, such as those below 0 °C, battery charge and discharge become increasingly difficult. Fig. 1 shows a simplified model that can be used to explain the problem for most types of batteries. V_o represents the open circuit voltage of the battery while R_c represents the resistance due to the ohmic voltage drop. The overvoltage resistance, R_{ov}, is used to represent the additional energy that must be supplied to get charge into or out of the battery [6,7]. As the temperature drops, R_{ov} increases because more energy is required to either charge or discharge the battery. R_{ov} is usually much larger than R_c, and therefore, at a sufficiently low temperature, it can be used to predict the internal temperature of the battery. However, it is also highly nonlinear with respect to the state-of-charge (SOC) and the magnitude and direction of the current, I_B. Therefore, SOC and I_B must be known while predicting R_{ov}. R_B represents the sum of R_{ov} and R_c.

* Present address: Erik Jonsson School of Engineering and Computer Science, University of Texas at Dallas, P.O. Box 830688, EC33, Richardson, TX 75083, USA. Tel: +1 972 883 6563; fax: +1 972 883 2710.
E-mail address: abhiman.hande@utdallas.edu.

0378-7753/$ – see front matter © 2005 Elsevier B.V. All rights reserved.
doi:10.1016/j.jpowsour.2005.11.027

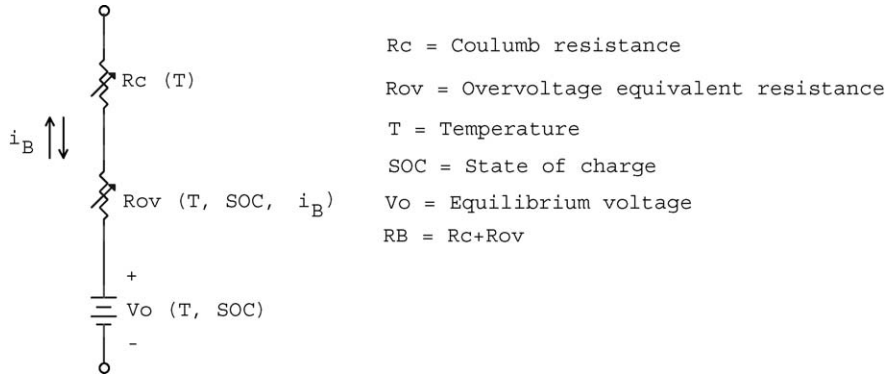

Fig. 1. Battery model.

3. Estimating internal battery temperature by measuring series battery resistance

3.1. Lead-acid batteries

In order to observe the behavior pattern of R_B with respect to internal battery temperature changes, tests were first performed on a Hawker Genesis G12V13AH VRLA battery with SOC = 67%. As the part number indicates, this is a 12 V_{DC} battery with a rated capacity of 13 ampere hours (Ah) at the 10 h discharge rate. This particular model was chosen because the same model also was available for comparative testing at Department of Energy's National Renewable Energy Laboratory (NREL). The following procedure was used to measure T_{bat} from R_B.

At 25 °C, an I_B equal to a fixed amplitude was applied for 2 s, and the battery voltage drop (ΔV_{bat}) was measured. Therefore, the series battery resistance (R_B) is given by

$$R_B = \frac{\Delta V_{bat}}{I_B}. \quad (1)$$

This process was repeated at 10, 0, −10, −20, −30 and −40 °C, after allowing the battery to soak for at least 4 h at each temperature. Therefore, after each temperature soak, T_{bat} can be assumed to be equal to the external ambient temperature. R_B was measured using I_B amplitudes of 50, 100, 200, 300, 400 and 500 A_{DC} at each temperature. R_B was found to vary with the amplitude of I_B and therefore, these different values of I_B were used for measuring R_B. The tests were performed using the AeroVironment ABC150 power processing system [8] to apply the 2 s I_B current pulse directly to the battery. The I_B pulse amplitude was accurately measured with a Hall effect sensor since the 2 s pulse was found to saturate all of the available current pulse transformers. Fig. 2 shows the experimental setup.

In order to obtain the ΔV_{bat} measurements, a second battery (V_s) was placed in series with the voltage probe to provide a 12 V_{DC} offset voltage. This was necessary to obtain a sufficiently high resolution for ΔV_{bat} on the scope. To provide a well-defined point on the decaying ΔV_{bat} pulse, the ΔV_{bat} and I_B values at the end of the pulse ($\Delta t = 2$ s) were used for all the R_B calculations.

ΔV_{bat} in all of the plots, such as Fig. 3, uses the 0 V_{DC} point as the reference. All the scope traces used a time scale

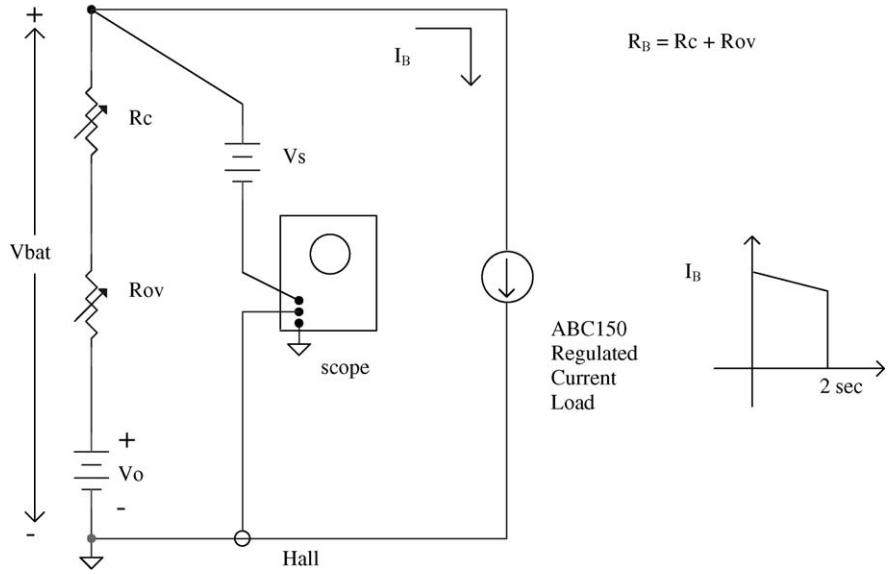

Fig. 2. Pulse discharge test circuit using the ABC150.

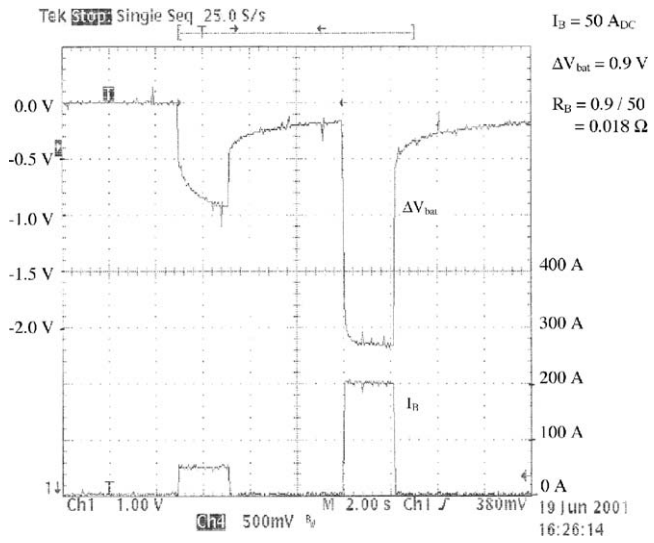

Fig. 3. R_B measurement at I_B = 50 and 200 A_{DC} at 25 °C.

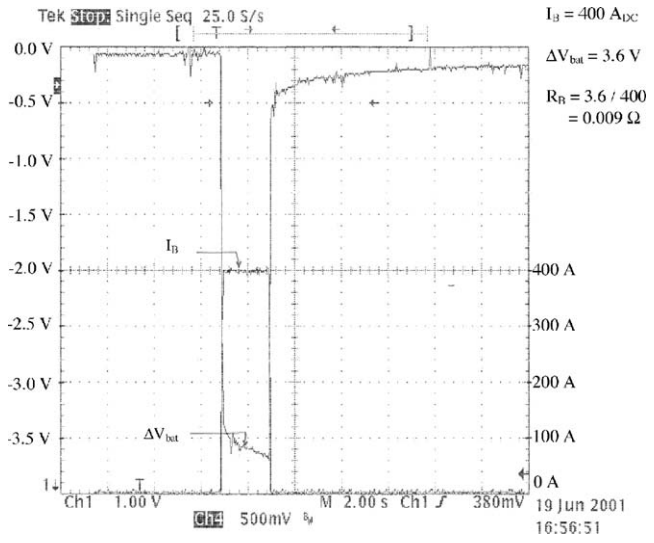

Fig. 5. R_B measurement at I_B = 400 A_{DC} at 25 °C.

of 2 s cm^{-1}. For the 10 to −40 °C measurements, a charge pulse of equal size was applied 5 s after the initial I_B discharge pulse. This was done to try to keep the SOC at about the same value throughout the tests. This pulse is beyond the range of the scope display, but it explains the abrupt increase in ΔV_{bat} at t = 7 s for all of these measurements. Because of the slow sweep speed, better results were obtained if the scope was triggered manually prior to applying the ABC150 pulse. However, this means that the pulse does not always start at the same point on the time scale.

Fig. 3 shows measurements at 50 and 200 A_{DC} at 25 °C, but only one pulse was used in subsequent measurements because of concern that the first pulse may start a chemical reaction in the battery that would affect the second pulse. Figs. 4 and 5 show pulse measurements at 25 °C with I_B = 300 and 400 A_{DC}, respectively, wherein the pulse amplitudes overlap, which is actually advantageous because it increases the measurement resolution. The maximum I_B amplitude of 520 A_{DC} in Fig. 6 is based on the maximum current pulse capability (MPCC) of the ABC150 which is 530 A_{DC}. From Fig. 6, at I_B = 520 A_{DC}, ΔV_{bat} =4.6 V.

$$\therefore R_B = \frac{\Delta V_{bat}}{I_B} = \frac{4.6}{520} = 0.0088\,\Omega.$$

Figs. 7 and 8 show two plots that depict the pulse measurements at 10 °C with I_B = 300 and 400 A_{DC}. At 10 °C, the battery could only supply a maximum I_B pulse of slightly over 400 A_{DC} instead of the 520 A_{DC} maximum at 25 °C. Similarly, at 0 °C the maximum I_B that could be reached was only about 360 A_{DC}. In the −10 to −40 °C temperature range, the maximum achievable I_B continued to decrease until it just barely reached 100 A_{DC} at −40 °C. The waveforms are similar to those for 10 °C.

The calculated values of R_B at different T_{bat} values were later plotted and are shown in Fig. 9. As expected, R_B increases as T_{bat} decreases due to the increase in R_{ov}. Less obvious is the decrease in R_B as I_B increases. However, it should be remembered that R_{ov} is not a Coulomb resistance, and so it may exhibit

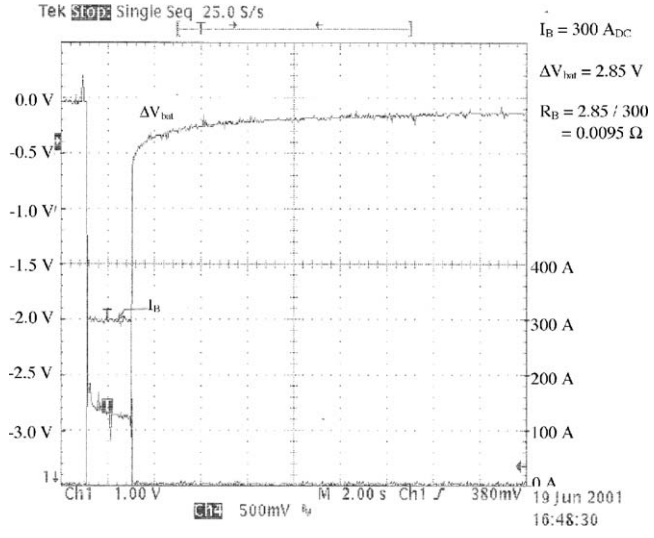

Fig. 4. R_B measurement at I_B = 300 A_{DC} at 25 °C.

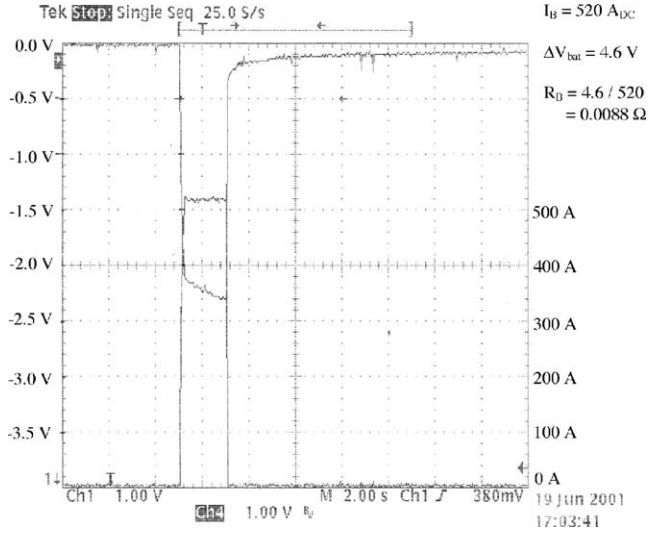

Fig. 6. R_B measurement at I_B = 520 A_{DC} at 25 °C.

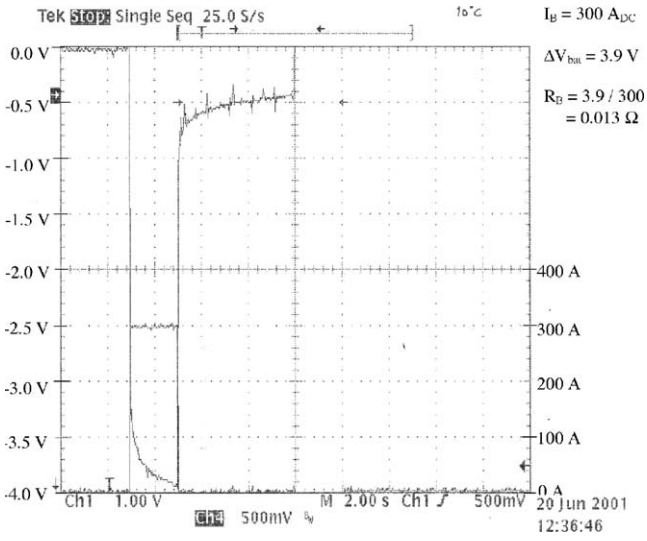

Fig. 7. R_B measurement at $I_B = 300\ A_{DC}$ at 10 °C.

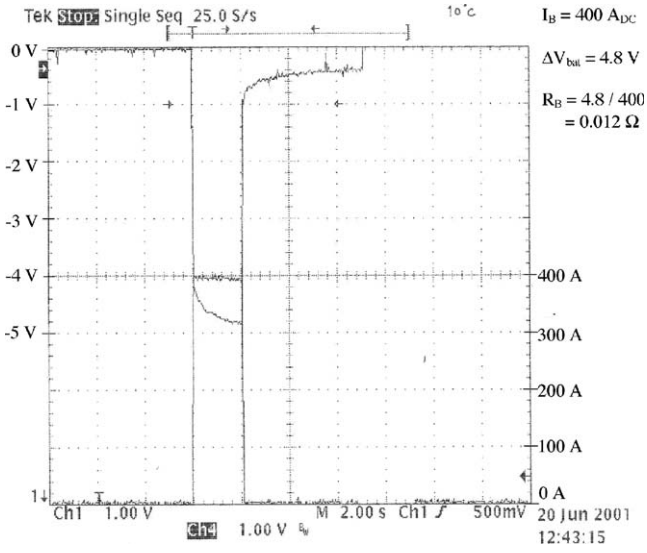

Fig. 8. R_B measurement at $I_B = 400\ A_{DC}$ at 10 °C.

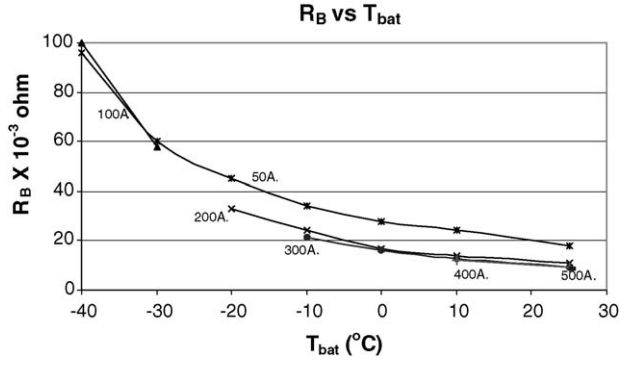

Fig. 9. R_B vs. T_{bat} for various pulse current amplitudes for the Hawker G12V13AH battery.

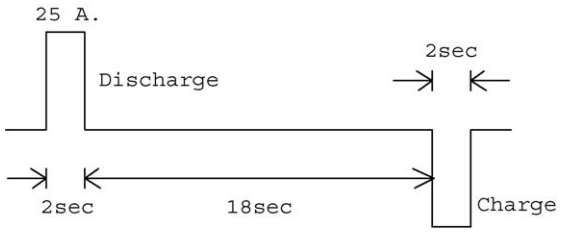

Fig. 10. I_B pulse used for measuring R_B for a single Panasonic NiMH battery.

a different form of behavior. Fig. 9 also indicates that for an I_B of fixed amplitude it may be possible to identify T_{bat}. These plots were later utilized during cold ambient temperature AC heating tests to predict the internal battery temperature as the batteries warmed up.

3.2. NiMH batteries

The behavior of R_B for T_{bat} changes was also studied for NiMH batteries. Experiments were conducted on an 8 V_{DC} 6.5 Ah Panasonic NiMH battery. R_B was measured using the ABC150 in a similar manner to that described in the previous section. A pulse waveform (I_B) having amplitudes of 25 A_{DC} 2 s^{-1} on both the discharge and charge cycles was applied in order to measure R_B. The waveform is shown in Fig. 10. The pulse test setup was similar to that used during the lead-acid battery tests (refer Fig. 2). Once again, if ΔV_{bat} equals the voltage drop during the I_B discharge cycle, $R_B = \Delta V_{bat}/I_B$. The I_B charge pulse was used to replace the charge taken during the discharge pulse.

Initially, an attempt was made to use a hybrid pulse power characterization (HPPC) type of pulse that had a discharge cycle of 6 A_{DC} for 18 s, a 32 s rest period and a 4.5 A_{DC} charge pulse for 10 s [9]. However, at 6 A_{DC}, V_{bat} was found to be too small to be accurately measured, especially at 25 °C. Therefore, a 25 A_{DC} pulse was used since the tests showed that this provided an adequate V_{bat} measurement.

R_B was measured after the batteries had been soaked for several hours at various temperatures from 25 to −30 °C. After a sufficiently long soak, the internal battery temperature can be assumed to be equal to its external ambient temperature, and this internal temperature was plotted versus R_B. These tests were repeated at various SOC values, and these plots were used to determine T_{bat} during the subsequent cold ambient temperature AC heating tests.

Table 1 shows the results obtained at various T_{bat} values. As expected, R_B increased with a decrease of temperature. However, it was almost constant for temperatures 25 °C and above, and therefore, it cannot be used to identify battery temperatures above 25 °C. Also, this test revealed that R_B is very insensitive to the SOC. Eventually, it was planned to test a 10–20 kHz heater [10,11] to warm a pack of 16 series connected Panasonic NiMH battery modules at different cold temperatures. Therefore, the values of R_B in Table 1 were multiplied by 16 and the resulting R_B values were plotted versus T_{bat} as shown in Fig. 11. This plot was used to predict T_{bat} from R_B measurements in subsequent AC heating tests.

Table 1
R_B (mΩ) vs. T_{bat} at different SOCs for a single Panasonic NiMH battery

T_{bat} (°C)	SOC (%)			
	25	55	75	100
45	11.2	11.2	11.2	9.6
35	11.2	11.2	11.2	11.2
25	14.4	12.8	14.4	11.2
10	22.4	20.8	22.4	20.8
0	27.2	25.6	27.2	28.8
−10	41.6	38.4	43.2	43.2
−20	65.6	64.0	70.4	64

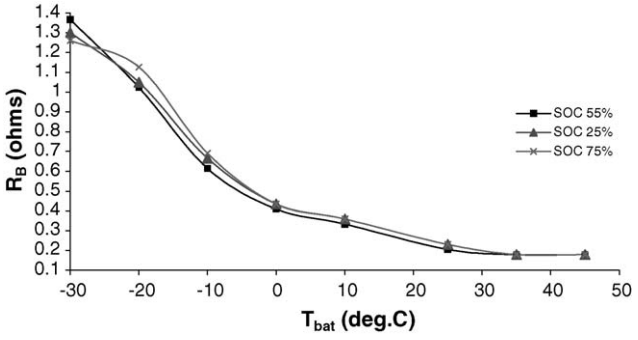

Fig. 11. R_B vs. T_{bat} at SOCs of 25, 55 and 75% for a 16 battery Panasonic NiMH pack.

4. Internal battery temperature prediction during cold temperature AC heating

4.1. Lead-acid batteries

After obtaining the necessary R_B versus T_{bat} plots for lead-acid batteries, experiments were conducted to heat these batteries at cold temperatures by using 60 Hz AC currents. The test results obtained while heating the Hawker Genesis G12V13AH VRLA battery with SOC ≅ 67% are explained in this section. The objective of the tests was to heat the battery by circulating 60 Hz AC currents at different cold temperatures and identify

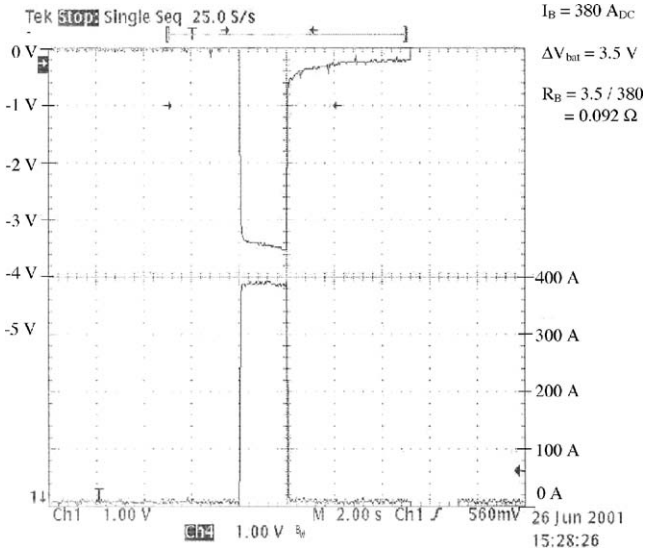

Fig. 13. R_B measurement at 25 °C using a reference MPCC pulse.

battery heating by measuring R_B using the results obtained in Fig. 9.

Before conducting this test, the maximum 2 s pulse current capacity [9] of the battery was determined at 25 °C with SOC ≅ 67%. This was done by programming the ABC150 to draw a pulse of 530 A_{DC}, which is its maximum capability. The ABC150 lower voltage limit was set at the minimum allowable battery voltage level of 8 V_{DC}. Therefore, the ABC150 will draw as much current as possible (MPCC) until the battery voltage ≤ 8 V_{DC}, as long as the MPCC ≤ 530 A_{DC}. The 2 s pulse width was chosen to be long enough to simulate the initial starting current of an electric motor. If only a few pulses are applied, e.g., less than 4 or 5, these pulses are short enough to have only a minor effect on the SOC.

Fig. 12 shows the test circuit. Since the connections for Fig. 12 created a higher series parasitic resistance than in Fig. 2, the maximum current amplitude became limited by this resistance instead of the ABC150. The waveform obtained is shown in

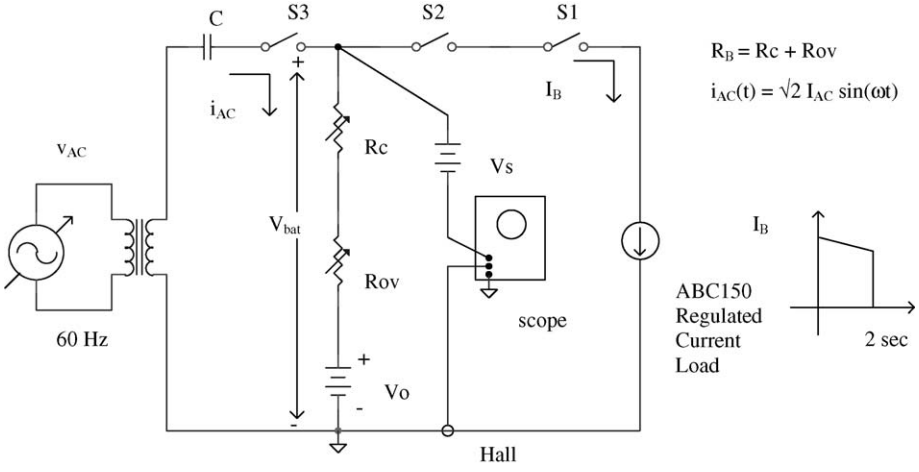

Fig. 12. Pulse discharge test circuit with 60 Hz AC heating.

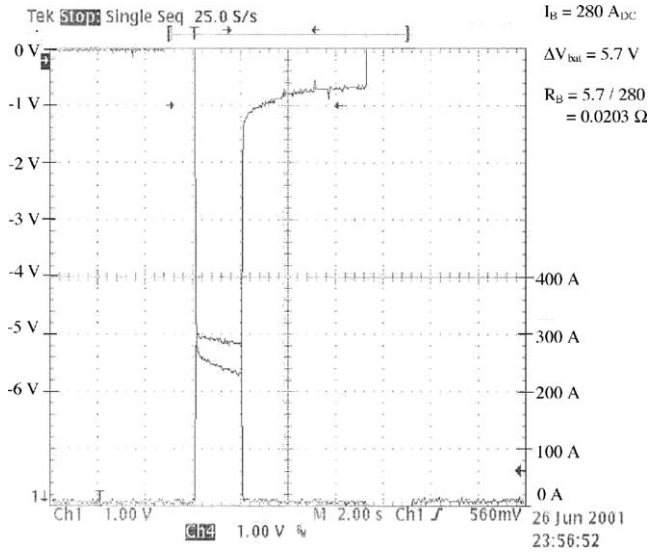

Fig. 14. R_B measurement at −20 °C using the MPCC test before AC heating.

Fig. 13. The MPCC equaled 380 A_{DC} and V_{bat} = 3.5 V_{DC}.

$$\therefore R_B = \frac{\Delta V_{bat}}{I_B} = \frac{3.5}{380} = 9.2\,\text{m}\Omega.$$

The battery was then soaked at −20 °C for 7 h. MPCC was applied again at this cold temperature, and I_B and V_{bat} were recorded using the digital storage scope. Fig. 14 shows the pulse test result. The MPCC equaled 280 A_{DC} and V_{bat} = 5.7 V_{DC}.

$$\therefore R_B = \frac{5.7}{280} = 20.3\,\text{m}\Omega.$$

The battery was then heated using 115 A_{rms}, 60 Hz AC currents for 3 min at −20 °C, and the pulse test in Fig. 15 indicated that R_B = 18 mΩ at 300 A_{DC}. Note that the AC current must be removed while applying MPCC pulse since it interferes with the MPCC waveform. Interpolating from the R_B data in Fig. 9, $T_{bat} \cong -6$ °C. Similarly, after 6 min of AC heating,

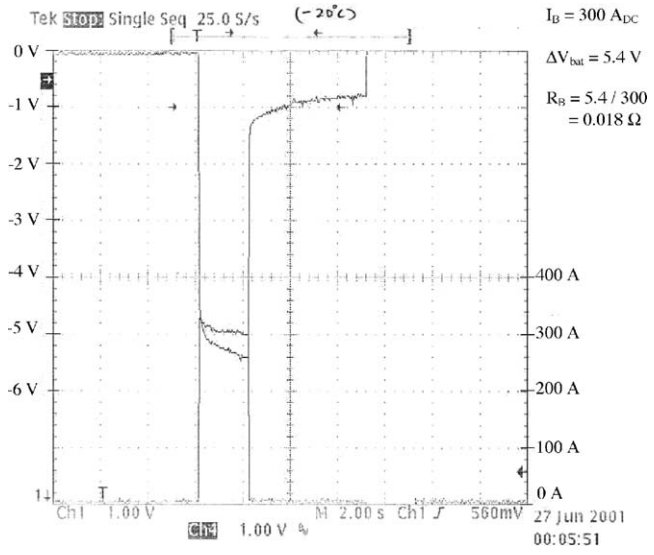

Fig. 15. R_B measurement at −20 °C using the MPCC test after 115 A_{rms} 60 Hz AC heating for 3 min.

Table 2
MPCC test data with 115 A_{rms} 60 Hz AC heating at −20 °C

AC heating (min)	R_B (mΩ)	I_B (A_{DC})	Estimated T_{bat} (°C)
None	20.3	280	−20
3	18.0	300	−6
6	10.9	320	+19
9	11.0	320	+19

Table 3
MPCC test data with 115 A_{rms} 60 Hz AC heating at −40 °C

AC heating (min)	R_B (mΩ)	I_B (A_{DC})	Estimated T_{bat} (°C)
None	108	100	−40
3	19.6	210	−4
6	14.7	250	+6
9	13.5	270	+9

R_B = 10.9 mΩ at 320 A_{DC}, and from Fig. 9, $T_{bat} \cong 19$ °C. After 9 min of AC heating, R_B = 11 mΩ at 320 A_{DC}, indicating that $T_{bat} \cong 19$ °C. The results for all heating periods are summarized in Table 2. This indicates a 14% increase in the maximum I_B after 6 min of heating, which is not a large improvement. However, it has been observed that the degree of improvement increases at lower temperatures and/or SOC levels. Table 2 also shows that T_{bat} begins to stabilize after 6 min.

Similar tests were conducted at other cold temperatures. The results obtained at −40 °C after soaking the battery for 8 h are tabulated in Table 3. The MPCC equaled just 100 A_{DC} and R_B equaled 108.3 mΩ after the 8 h −40 °C soak. After 3 min of 115 A_{rms} 60 Hz heating, MPCC equaled 210 A_{DC} indicating that R_B = 19.6 mΩ. Interpolating from the R_B data in Fig. 9, $T_{bat} \cong -4$ °C. This indicates a 110% increase in the maximum I_B after 3 min of heating, which is a significant improvement. After 6 min of AC heating, R_B = 14.7 mΩ at 250 A_{DC}, and from Fig. 9, $T_{bat} \cong 6$ °C. After 9 min of AC heating, R_B = 13.5 mΩ at 270 A_{DC}, indicating that $T_{bat} \cong 9$ °C.

During 115 A_{rms} AC heating, the AC power ($P_{bat} = 115^2 \times R_B$) was recorded at specified time intervals as well. As expected, P_{bat} decreased with time as the electrolyte warmed up as shown in Fig. 16.

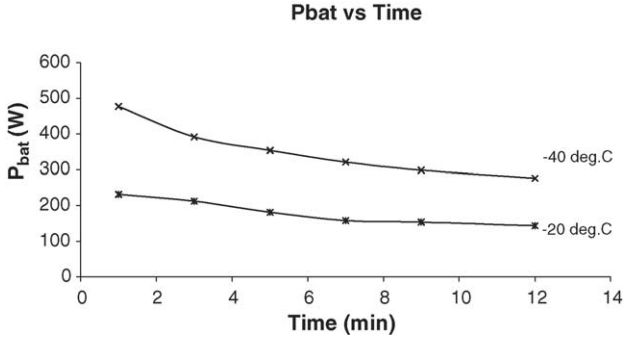

Fig. 16. P_{bat} ($I_{rms}^2 R_B$) vs. time for ambient temperatures of −20 and −40 °C.

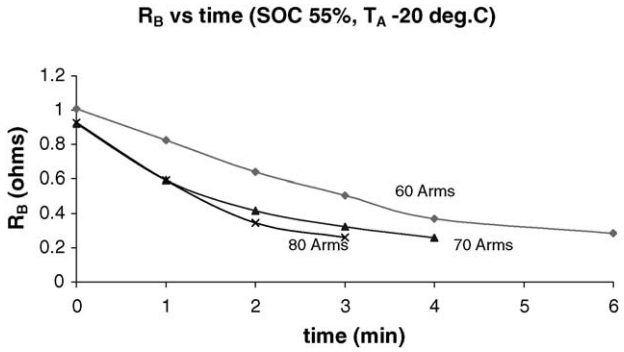

Fig. 17. R_B vs. time results at −20 °C with SOC ≅ 55%.

4.2. NiMH batteries

The R_B versus T_{bat} graphs shown in Fig. 11 were later utilized to predict T_{bat} during cold temperature 10–20 kHz AC heating tests on the 16 series connected Panasonic NiMH battery pack. Measurements were made with the aid of the ABC150 Remote Operating Software (ROS) [12] using a personal computer. The data acquisition was carried out using a National Instruments PCI-6024E NI-DAQ card [13] that interfaced with a 16 channel Analog Devices 5B Series signal conditioning module [14]. Eight channels were used for measuring the eight pairs of battery voltages using Analog Devices 5B41 signal conditioning modules [15] and the remaining eight were used to measure the battery case temperatures using Analog Devices 5B37 signal conditioning modules [16].

Figs. 17 and 18 show the results after soaking the battery pack for at least 5 h at −20 °C with an SOC ≅ 55% [3]. Before applying the AC, $R_B \cong 1\,\Omega$. Interpolating from the R_B data in Fig. 11, $T_{bat} \cong -20\,°C$. R_B decreased to about 0.3 Ω after 6 min of 60 A_{rms} 10 kHz AC circulation, and from Fig. 11, $T_{bat} \cong 15\,°C$. As expected, when the amplitude of AC was increased the heating process sped up. From Fig. 18, it can be seen that with 70 A_{rms} AC circulation, 4 min were needed to heat the pack to about 18 °C, and with 80 A_{rms}, only 3 min were needed.

Figs. 19 and 20 show the results obtained after soaking the battery pack for 5 h at −30 °C with an SOC ≅ 55% [3]. Before applying the AC, $R_B \cong 1.3\,\Omega$ which corresponded to $T_{bat} \cong -30\,°C$. R_B decreased to about 0.3 Ω after 7 min of 60 A_{rms} 10 kHz AC circulation, and from Fig. 11, $T_{bat} \cong 14\,°C$.

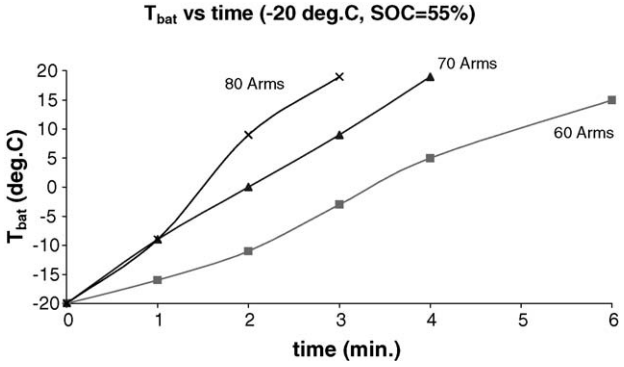

Fig. 18. T_{bat} vs. time results at −20 °C with SOC ≅ 55%.

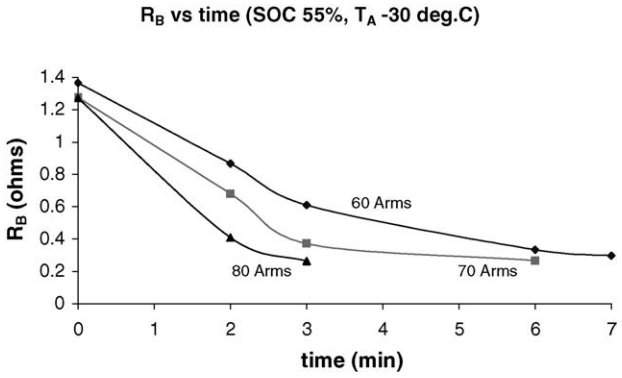

Fig. 19. R_B vs. time results at −30 °C with SOC ≅ 55%.

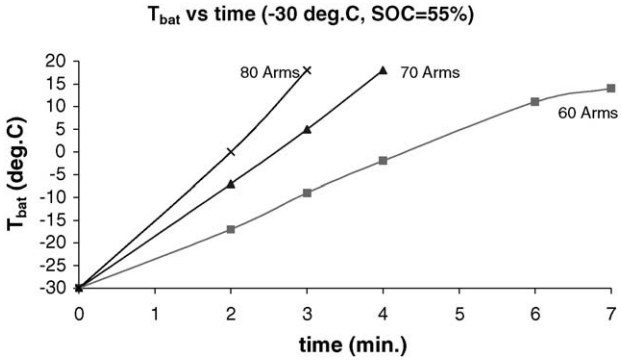

Fig. 20. T_{bat} vs. time results at −30 °C with SOC ≅ 55%.

However, the results for 70 and 80 A_{rms} were about the same as those for −20 °C, i.e., with 70 A_{rms} AC circulation, 4 min were needed to heat the pack to about 18 °C, and with 80 A_{rms}, 3 min were needed (refer Fig. 20).

In order to observe the effects of AC heating at different SOCs, tests were conducted at SOCs of 25, 55 and 75% using 10 kHz AC at an amplitude of 60 A_{rms}. Figs. 21 and 22 show the results obtained after soaking the pack for 5 h at −30 °C with SOCs of 25, 55 and 75% [3]. In this case, about 6 min were needed to heat the pack to about 15 °C when the pack SOC was 75%, but more time was needed when the SOC was lower. As shown by the plots for SOC = 55%, T_{bat} was about 13 °C after 7 min and for SOC = 25% T_{bat} was about 12 °C after 8 min.

During all of these AC heating tests it was observed that the case temperatures were slightly lower than the extrapolated T_{bat}

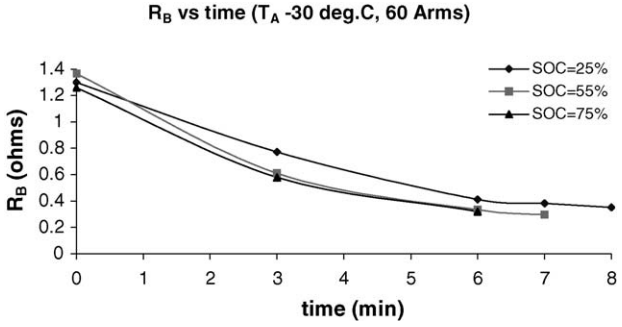

Fig. 21. R_B vs. time results at −30 °C with 60 A_{rms} AC heating.

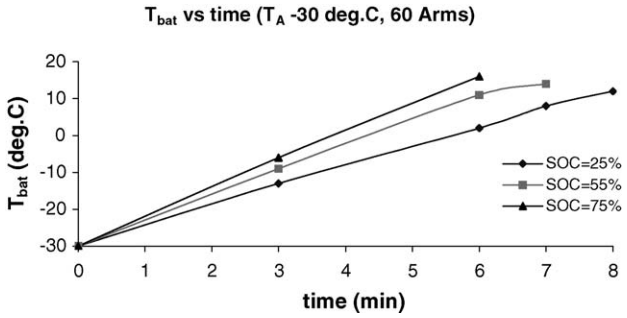

Fig. 22. T_{bat} vs. time results at −30 °C with 60 A_{rms} AC heating.

estimations using R_B. This means that the electrolyte temperature was higher than the case temperature. However, the accuracy of these temperature estimations using R_B measurements has yet to be verified and this area deserves further study.

5. Conclusions

Preliminary tests have shown that it is possible to predict the internal battery temperature for both lead-acid and NiMH batteries during cold temperature AC heating by measuring R_B. Initial tests were conducted on a Hawker Genesis G12V13AH VRLA battery with SOC ≅ 67%. Data for R_B versus T_{bat} were calculated from a series of tests using a 2 s pulse at various battery currents (I_B). The intent of this data was to use R_B to estimate T_{bat} in later experiments where AC heating was applied. However, the accuracy of this technique has not been verified since the battery had no internal temperature sensors to check the results. As expected, when the battery was soaked at a cold temperature, R_B increased as T_{bat} decreased. In addition, there was a decrease in R_B at higher values of I_B. In spite of this effect, it is quite obvious that for an I_B of fixed amplitude it is possible to identify the approximate internal battery temperature at cold ambient temperatures.

In the next series of tests, the characteristics of a 2 s pulse load were evaluated before and after AC heating was applied. Tests at −20 °C indicated that the battery actually worked reasonably well even before the AC was applied, but the AC still provided significant improvement. At −40 °C, the battery performed very poorly before the AC heating and provided a pulse of only 100 A_{DC}. This increased to 210 A_{DC} after 3 min of 115 A_{rms} 60 Hz AC heating and to 250 A_{DC} after 6 min.

Similar tests were also conducted on 8 V_{DC} 6.5 Ah Panasonic NiMH batteries. Some battery experts indicated that each 60 Hz AC half cycle could be enough time for battery ionization to occur, i.e., the charge process might be initiated during each alternate 8.33×10^{-3} s half cycle, and this could contribute to a decrease in battery lifetime. Therefore, these tests were conducted using a high-frequency 10–20 kHz heater [10,11]. Suitable plots of R_B versus T_{bat} were plotted at different SOCs for a pack of 16 series connected Panasonic batteries. These plots were used to investigate the effect of 10–20 kHz AC on cold temperature battery performance. Tests showed that at both −20 and −30 °C, 10–20 kHz AC currents at amplitudes of 60–80 A_{rms} can restore the battery resistance and temperature to values close to those at 25 °C within a few minutes. As expected, the heating process sped up as the amplitudes of the AC was increased.

Acknowledgements

This research was supported by grants from DaimlerChrysler, AG and the U.S. Department of Energy National Renewable Energy Laboratory (NREL), and was conducted at University of Toledo's Power Electronics Laboratory (PEL) under subcontract no. ACI-9-29118-01. The author would like to acknowledge the advice and assistance provided by Dr. Thomas Stuart (co-director of PEL) and Dr. Ahmad Pesaran (NREL).

References

[1] T. Stuart, A. Hande, AC battery heating for cold climates, in: Proceedings of the EnV 2001 Conference, Engineering Society of Detroit, Southfield, MI, June 10–13, 2001.
[2] T. Stuart, A. Hande, AC heating for EV/HEV batteries, in: 7th IEEE Workshop on Power Electronics in Transportation (WPET 2002) Conference, Detroit, MI, October 24–25, 2002.
[3] T. Stuart, A. Hande, HEV battery heating using AC currents, J. Power Sources 129 (April (2)) (2004) 368–378.
[4] A. Hande, T. Stuart, Effects of high frequency AC currents on cold temperature battery performance, in: Proceedings of the 2nd IEEE India International Congress on Power Electronics (IICPE 2004), Mumbai, India, December 20–21, 2004.
[5] A. Pesaran, A. Vlahinos, T. Stuart, Cooling and preheating of batteries in hybrid electric vehicles, in: Proceedings of the 6th ASME-JSME Thermal Engineering Joint Conference, Hawaii Island, Hawaii, March 16–20, 2003.
[6] D. Berndt, Maintenance-free Batteries, second ed., Research Studies Press Ltd., Taunton, England, 1997.
[7] D. Rand, R. Woods, R. Dell, Batteries for Electric Vehicles, Research Studies Press Ltd., Taunton, England, 1998.
[8] ABC150 Power Processing System, AeroVironment Inc., 2005, http://www.aerovironment.com/area-pps/prod-serv/abc-150.html.
[9] PNGV Battery Test Manual, DOE/ID-10597, Revision 3, February 2001.
[10] C. Ashtiani, T. Stuart, Circulating Current Battery Heater, U.S. Patent 6,259,229, July 10, 2001.
[11] A. Hande, A high frequency inverter for cold temperature battery heating, in: Proceedings of the 9th IEEE Workshop on Computers in Power Electronics (COMPEL'04) Conference, University of Illinois, Urbana-Champaign, IL, August 15–18, 2004, pp. 215–223.
[12] ABC150 Remote Operating System Manual, Revision 1.0, AeroVironment Inc., August 1998.
[13] Low-Cost E Series Multifunction DAQ 12 or 16-Bit, 200 kS/s, 16 Analog Inputs, National Instruments Corporation, 2004, http://www.ni.com/pdf/products/us/4daqsc202-204_ETC_212-213.pdf.
[14] 5B Series Signal Conditioning Modules, Analog Devices, 2005, http://www.analog.com/en/content/0,2886,774%255F868%255F46551,00.html.
[15] 5B41 Isolated Voltage Input Signal Conditioning Modules, Analog Devices, 2005, http://www.analog.com/UploadedFiles/Data_Sheets/90194225B40_41_0.pdf.
[16] 5B37 Isolated Thermocouple Input Signal Conditioning Modules, Analog Devices, 2005, http://www.analog.com/UploadedFiles/Data_Sheets/102187305B37_0.pdf.